

Preparation of nano-TiO₂/purified diatomite coating and its photocatalytic properties of formaldehyde degradation

Lijian Wang^a, Junwei Zhao^a, Yujiang Wang^a and Shuilin Zheng^{b,*}

^aMaterials Science and Engineering School & Henan Key Laboratory of Special Protective Materials, Luoyang Institute of Science and Technology, Luoyang 471023, P. R. China

^bSchool of Chemical and Environmental Engineering, China University of Mining and Technology, Beijing 100083, P. R. China

The nano-TiO₂/purified diatomite composite materials with core-shell structures were prepared by hydrolysis precipitation using purified diatomite as carrier and titanium sulfate as precursor. The composite materials were characterized by transmission electron microscope (TEM), X-ray diffraction (XRD), low temperature nitrogen adsorption and mercury porosimetry. The photocatalytic composite coating based on the nano-TiO₂/purified diatomite composite materials was prepared and its properties of formaldehyde degradation were investigated. Meanwhile, the degradation mechanism of formaldehyde gas was discussed. The results showed that the nano-TiO₂/purified diatomite composite materials were formed core-shell structures, and the TiO₂ nanoparticles were anatase with the average size of about 10 nm. The test results show that the formaldehyde purification performance of the coatings has met the technical requirements of Class I materials in the Chinese national standard JC/T 1074-2008.

Key words: Nano-TiO₂/purified diatomite, Photocatalytic coating, Degradation, Formaldehyde gas.

Introduction

With the improvement of people's living standard and health consciousness, the materials of green environmental protection for interior decoration become more and more popular. The conventional decorative materials will gradually release hazardous substances such as formaldehyde after decoration [1, 2]. Therefore, the indoor gas pollution has become an urgent problem to be solved. Study on the environmentally friendly interior decoration materials is significant in academia as well as application. Formaldehyde, as a common indoor air pollution chemical, poses a serious threat to people's health [3, 4]. At present, the methods of removing indoor formaldehyde include physical adsorption, plant absorption and purification, windowing ventilation, air purification and catalytic degradation. In recent years, the photocatalytic degradation method has become available to purify indoor formaldehyde due to its low energy consumption, simple operation, mild reaction conditions and the ability to reduce secondary pollution [5, 6]. However, the traditional methods of adsorption or chemical degradation are not effective in the degradation of formaldehyde or cause secondary pollution. Therefore, it is urgent to develop economical and efficient formaldehyde reduction strategy. Semiconductor

photocatalysis belongs to a new technology for environmental pollution control. The electronic structures of various semiconductor metal oxides and sulfides as catalysts make them exhibit excellent photocatalytic activity. Nanoscale titanium dioxide (Nano-TiO₂) is one of the most studied photocatalytic materials [7-14]. The nano-TiO₂ advantages of photocatalytic degradation of formaldehyde include strong oxidation ability, complete degradation and no secondary pollution [5]. However, the poor dispersion of nano-TiO₂ limits its application in decorative materials. In order to improve the photocatalytic ability, the nano-TiO₂ coated large porous materials with high specific surface area have been studied [15]. The obtained composites can not only prevent the aggregation of fine nano-TiO₂ particles, but also improve the photodecomposition performance [16]. In recent years, various porous materials have been developed as carriers of nano-TiO₂ [17-20]. Because of the larger specific surface area, these carriers actually increase the local concentration of organic compounds and avoid volatilization or dissociation of intermediate products. Correspondingly, the photocatalyst reaction rate was accelerated [21, 22].

Diatomite is a kind of siliceous and biogenic siliceous sedimentary rock, which is mainly composed of the remains of ancient diatoms. The main chemical composition of diatomite is SiO₂. The relative density of pure and dry diatomite is 0.4-0.9 g/cm³, and the pore size distribution is 50-800 nm. The multifunctional composites can be constructed by using the natural pores of diatomite [6, 23-27].

*Corresponding author:
Tel : +8637965928196
Fax: +8637965928196
E-mail: shuilinzheng8@gmail.com

In this study, the nano-TiO₂/purified diatomite composite materials were firstly synthesized by typical hydrolytic precipitation method using titanate sulphate as precursor. And then, the novel photocatalytic coating was innovatively developed based on the prepared nano-TiO₂/purified diatomite composite materials, which can effectively degrade indoor formaldehyde gas. The photocatalytic activity of the nano-TiO₂/purified diatomite coating was studied through the photocatalytic degradation of formaldehyde with a white light source.

Material and methods

Materials and reagents

Diatomite powder was purchased from Meiston Powder Material Co., Ltd. (Linjiang City, Jilin Province). Titanate sulphate (Ti(SO₄)₂) was purchased from Jingxiang Chemical Plant (Changping, Beijing). All the chemicals used in the experiment were analytical pure. The deionized water was prepared in laboratory, which has a resistivity not less than 18.2 MΩ.

Purification of diatomite

In order to eliminate the influence of impurities on the properties of synthetic materials, diatomite was firstly purified. Diatomite (10.0 g) was calcined at 550 °C for one hour, and then immersed in 50% sulphuric acid solution (40.0 g) for 2 h. After centrifuging and washing twice with water, the purified diatomite was obtained.

Preparation of nano-TiO₂/purified diatomite composite materials

In an ice water bath, the purified diatomite and deionized water with a mass ratio of 1:24 were placed in a beaker under vigorous stirring. And then the diluted sulfuric acid was added to adjust the pH of the solution to 3. After that, the Ti (SO₄)₂ solution (3.0 mol/L, 10 mL) was slowly dripped by a constant current pump. Ti (SO₄)₂ was used as titanium source. Then, the ammonium sulphate solution (1.5 mol/L, 20 mL) was pumped into the beaker. After continuous mixing for half an hour, the above mixed solution was heated to 40 °C and remained at this temperature for half an hour. The pH value of the mixture was adjusted to 5.5 with diluted ammonia solution. After one hour of continuous reaction, the white precipitate was collected by centrifuging, filtration, washing, drying and calcination at 650 °C for 2 h. The nano-TiO₂/purified diatomite composite materials were prepared. The preparation process was shown in Fig. 1.

Preparation of photocatalytic coating

Deionized water (302.0 g), sodium acrylate salt water dispersant (5.0 g), defoamer (F111, 2.0 g) and film-forming additives (5.0 g) were added to a beaker in turn. After being uniform stirred for 5 min, some nano-

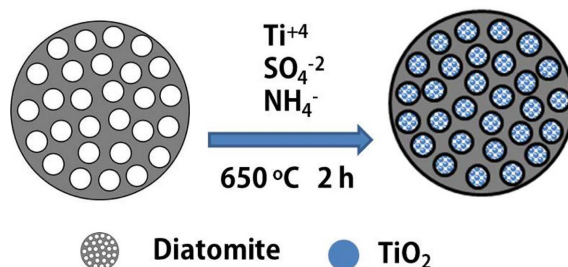


Fig. 1. Preparation schematic diagram of the nano-TiO₂/purified diatomite composite materials.

TiO₂/purified diatomite composite materials (48.0 g) were slowly added. At a speed of 2000 r/min, the waterborne colloid was obtained by stirring and dispersing for half an hour. The pigments and fillers of calcined kaolin (100.0 g), light calcium carbonate (100.0 g) and talcum powder (100.0 g) were added into the waterborne colloid by vigorous stirring for half an hour and then styrene acrylate emulsion (110.0 g) was added by mild stirring. The pH value of the mixed system was adjusted to 8 with neutralizer. Finally, thickener (ASE-60, 5.0 g) and levelling agent (RM-2020, 10.0 g) were added with stirring evenly and aging for one hour. The prepared nano-TiO₂/diatomite photocatalytic coating was obtained.

Characterization

The samples for TEM observation were fabricated by RTO metal-embedded chip micron-nano characterization method. First, the powder particles were embedded in copper by ion deposition without disturbance, and then the samples were thinned to nanometer thickness by mechanical grinding, polishing and ion shearing. The samples were analyzed by Hitachi H-800 Microscope for image analysis to observe the profile of nano-TiO₂ coated on the surface of diatomite particles. The crystal structure of nano-TiO₂ was analyzed by Brooke X-ray diffractometer (XRD). The pore size and pore volume were measured by NOVA4000 high-speed automatic specific surface and porosity meter produced by Conta Company and Autopore IV 9500 mercury intrusion meter produced by Mike Company in the United States, and the specific surface area of samples was measured by ST-2000 of Beijing Beibu Instrument Technology Company.

Photocatalytic coating for degradation of formaldehyde gas

The formaldehyde gas purification performance of the photocatalytic coatings was tested by entrusting National Building Material Industry Technology Monitoring and Research Center of China based on JC/1074-2008 "Cleaning Performance of Indoor Air Purification Functional Coatings". The detection process was as follows: First, the indoor environment was simulated by the environment test chamber under the visible

white light source. The temperature was set at 23 ± 0.5 °C and the humidity was set at $45 \pm 3\%$. Second, the formaldehyde solution with a concentration of 37% - 40% at 2.5 μL was dripped onto a petri dish and put into the environmental test chamber to make it fully volatilized in the environmental test chamber. Third, the photocatalytic coating was coated on 0.1 m² glass (250 g/m², twice), and irradiated by white fluorescent light source (30 W) to produce photocatalytic effect. The distance between the light source and the sample was 70 cm. Fourth, acetylacetone spectrophotometry (GB/T 15516-1995) was used to detect the concentration of formaldehyde. The gas in the 10 L cabin was sampled every 6 h to detect the change of formaldehyde concentration in the environmental test cabin. Fifth, the control group was conducted in another environmental chamber. According to the above experimental steps, the glass plate is not coated with photocatalytic coating in step 3.

Results and Discussion

Fig. 2 shows the TEM of cross-section of the nano-TiO₂/purified diatomite composite materials. Fig. 2(a) is a TEM image of the RTO profile of nano-TiO₂ loaded on the surface of a circular sieve diatomite. Fig. 2(b) is a locally magnified image of the interface between nano-TiO₂ and diatomite. It can be seen from Fig. 2(b) that the prepared nano-TiO₂/purified diatomite composites show obvious core-shell structure with diatomite as core and nano-TiO₂ as shell. The core-shell structure is closely bonded with each other. The thickness of the coated shell is about 230 nm. The micropores on the surface of diatomite have been covered by nano-TiO₂, and the macropores on the surface are clearly observed.

Fig. 3 is a magnified TEM image of point A in Fig. 2(b). The average size of titanium dioxide at point A is about 10 nm. Fig. 4 is the result of energy spectrum analysis at point B in Fig. 1(b), where is the interface between titanium dioxide and diatomite. The peaks of Si and Ti elements can be observed in the spectrum. It is further proved that the nano-TiO₂/purified diatomite composite materials is formed.

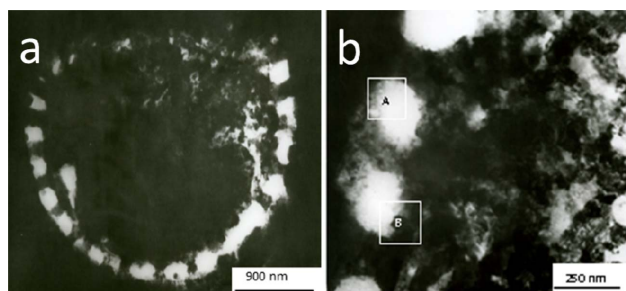


Fig. 2. TEM of cross-section of the nano-TiO₂/purified diatomite composite materials.

The synthesized nano-TiO₂/purified diatomite composite materials were analyzed by XRD. In the previous work, the temperature of crystalline phase transformation of TiO₂ in the composite powder is about 800 °C [25]. Therefore, in this work, the synthesized nano-TiO₂/purified diatomite composite materials were calcined at 650 °C for 2 h. The results are shown in Fig. 5. The diffraction peaks of the prepared samples are 25.2, 37.7

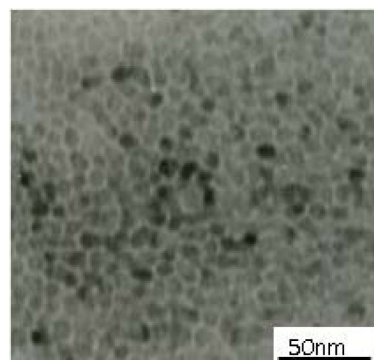


Fig. 3. The magnified TEM of point A in Fig. 2(b).

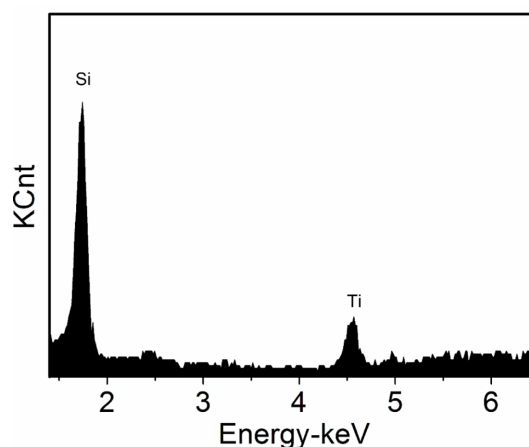


Fig. 4. EDS spectrum of the nano-TiO₂/purified diatomite composites.

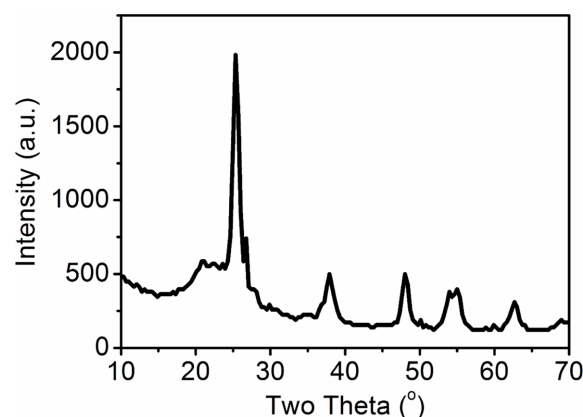


Fig. 5. XRD patterns of the nano-TiO₂/purified diatomite composite materials.

and 48.0 degrees, which are matched well with the standard spectra of anatase-type titanium dioxide (JCPDS71-167). This indicates that the crystal structure of titanium dioxide loaded on the surface of diatomite is anatase. The average single crystal size of the sample can be calculated by Scherrer formula: $D = K\lambda/B\cos\theta$, where K is Scherrer constant, $K = 0.89$, $\lambda = 0.15406$ nm and B is the half-width of the crystal plane with the strongest diffraction peak (101). The average size of the loaded titanium dioxide is about 11 nm, which is consistent with that observed by TEM.

The pore size and specific surface area of the purified diatomite and the nano-TiO₂/purified diatomite composite materials were determined by low temperature nitrogen adsorption and mercury porosimetry, respectively, which are summarized in Table 1. The results of nitrogen adsorption at low temperature show that the mesoporous volume and specific surface area of the nano-TiO₂/purified diatomite composite materials are significantly higher than that of the purified diatomite, while the average pore size is significantly lower than that of the purified diatomite. These results indicate that the nano-TiO₂/purified diatomite composite materials own mesoporous structure. The results of mercury intrusion test show that the average pore size of the nano-TiO₂/purified diatomite composite materials become lower, which further indicate that the inner surface of the larger pore of purified diatomite was loaded with nano-TiO₂.

The formaldehyde gas purification performance of the photocatalytic coating was tested by entrusting National Building Material Industry Technology Monitoring and

Research Center of China. The test results of formaldehyde gas degradation are shown in Fig. 6. As shown in Fig. 6, the degradation rate of the photocatalytic coating increases gradually with the prolongation of irradiation time. After 48 h of illumination, the degradation rate of the photocatalytic coating reached 82.8%, which meets the technical requirements of Class I materials in the standard JC/T 1074-2008 of China. Correspondingly, the control group without the photocatalytic coating had lower photocatalytic degradation rate.

It is well known that the degradation rate of substrates in photocatalytic reactions was achieved by adsorbing on the surface of catalysts or reaching the surface of catalysts of free molecules [28]. In our case, the main mechanism of formaldehyde gas degradation in photocatalytic coating is that the molecules of formaldehyde gas were adsorbed on the surface of the coatings firstly, and then were oxidized and degraded by the catalyst in the coating under irradiation of fluorescent light source. The prepared photocatalytic coating consists of the nano-TiO₂/purified diatomite composite materials, which increase the adsorption of the coating. The adsorption effect enriches formaldehyde and other pollutants in the air onto the surface of the photocatalytic coating, thus accelerating the degradation of pollutants by accepting electrons and holes directly on the surface of the nano-TiO₂/purified diatomite.

Fig. 7 is a schematic diagram of the photocatalytic degradation mechanism of formaldehyde by the nano-TiO₂/purified diatomite composites with core-shell structures. In Fig. 7, the photon energy which is greater

Table 1. The pore size and specific surface area of the purified diatomite and the nano-TiO₂/purified diatomite composite materials.

Materials	Low Temperature Nitrogen Adsorption Method			Mercury Porosimetry
	Pore volume (mL/g)	Average pore size (nm)	Specific surface area (m ² /g)	Average pore size (nm)
Purified diatomite	4.73×10^{-2}	60.56	31.26	285.1
Nano-TiO ₂ /purified diatomite	8.26×10^{-2}	10.2	32.39	251.2

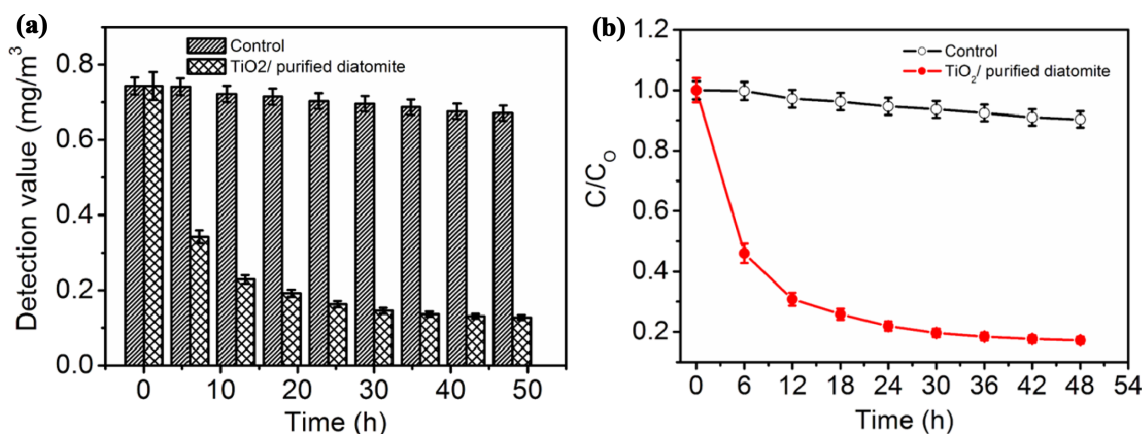
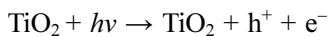
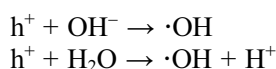


Fig. 6. The test results of formaldehyde gas degradation with and without the photocatalytic coating, respectively.

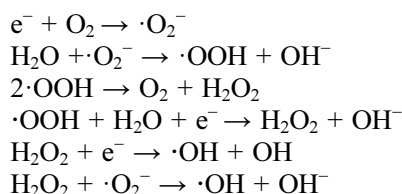
than the band gap of titanium dioxide (3.2 eV) directly excite electrons transition from the top of valence band to the bottom of conduction band, resulting in the formation of electron and hole pairs of nano-TiO₂ in photocatalytic coating:



Photogenerated holes can react directly with pollutants already adsorbed on the surface of coating and oxidize them, or react with hydroxyl groups and water to produce hydroxyl radicals $\cdot\text{OH}$.



Photogenerated electrons react with oxygen molecules adsorbed on the coating surface to produce superoxide radicals. Molecular oxygen not only participates in the reduction reaction, but also is another source of hydroxyl radicals on the surface. The specific reaction formulas are as follows:



In the above reaction, hydroxyl radicals ($\cdot\text{OH}$) and superoxide radicals ($\cdot\text{O}_2^-$) have been produced. They are very active free radicals with strong oxidation ability, which can directly oxidize various organic substances to small inorganic molecules such as CO₂ and H₂O. Moreover, the oxidation reaction generally does not stop in the intermediate step and does not produce intermediate products because of their strong oxidation ability. The above analysis shows that the

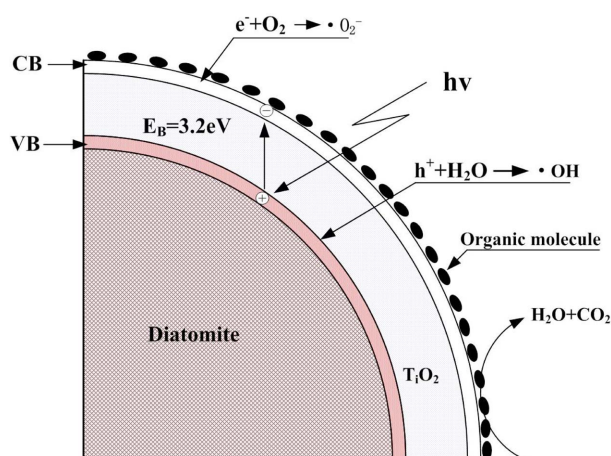


Fig. 7. Schematic diagram about the photocatalytic degradation mechanism of the nano-TiO₂/purified diatomite coating.

degradation of formaldehyde gas is determined by the adsorption and photocatalytic degradation properties of the nano-TiO₂/purified diatomite coating, and the degradation effect is the result of the synergistic effect of the two.

Conclusion

The nano-TiO₂/purified diatomite composites were prepared by hydrolytic precipitation method using purified diatomite as carrier and titanium sulfate as precursor. The nano-TiO₂/purified diatomite composite particles show obvious core-shell structure with diatomite as core and nano-TiO₂ as shell. The nano-TiO₂/purified diatomite photocatalytic coating was prepared by using the prepared nano-TiO₂/purified diatomite composite as filler. The test results of the formaldehyde degradation performance of the coating show that the formaldehyde degradation performance of the coating has met the technical requirements of Class I materials in the national standard JC/T 1074-2008 of China. The degrading effect of photocatalytic coating on formaldehyde gas is the result of the synergistic effect of adsorption and photocatalytic degradation.

Acknowledgements

This work was supported by 135 National Key R&D Program Projects of the Ministry of Science and Technology (2016YFC0700901) and the Opening Foundation of Henan Key Laboratory of Special Protective Materials (Grant No. SZKFJJ201903).

Competing Financial Interests

The authors declare no competing financial interests.

References

1. K.-S. Liu, F.-Y. Huang, S.B. Hayward, J. Wesolowski, and K. Sexton, *Environ. Health Perspect.* 94 (1991) 91-94.
2. C.H. Ao, S.C. Lee, J.Z. Yu, and J.H. Xu, *Appl. Catal., B* 54 (2004) 41-50.
3. O. Merk and G. Speit, *Environ. Mol. Mutagen.* 32[3] (1998) 260-268.
4. C.W. Kim, J.S. Song, Y.S. Ahn, S.H. Park, J.W. Park, J.H. Noh, and C.S. Hong, *Yonsei Med. J.* 42 (2001) 440-445.
5. A. Fujishima, T.N. Rao, and D.A. Tryk, *J. Photochem. Photobiol., C* 1 (2000) 1-21.
6. Q. Sun, H. Li, S. Zheng, and Z. Sun, *Appl. Surf. Sci.* 311 (2014) 369-376.
7. N. Uekawa, M. Suzuki, T. Ohmiya, F. Mori, Y.J. Wu, and K. Kakegawa, *Int. J. Mater. Res.* 18[4] (2003) 797-803.
8. H. Choi, E. Stathatos, and D.D. Dionysiou, *Thin Solid Films* 510 (2006) 107-114.
9. A. López, D. Acosta, A. I. Martínez, and J. Santiago, *Powder Technol.* 202 (2010) 111-117.
10. X.Z. Li, H. Liu, L.F. Cheng, and H. J. Tong, *Environ. Sci. Technol.* 37[17] (2003) 3989-3999

11. S. Narakaew, *J. Ceram. Process. Res.* 18[1] (2017) 36-40.
12. A. Maddu, I. Deni, and I. Sofiana, *J. Ceram. Process. Res.* 19[1] (2018) 25-31.
13. Y.-S. Song, M.-H. Lee, B.-Y. Kim, and D.Y. Lee, *J. Ceram. Process. Res.* 20[2] (2019) 182-186.
14. Y.-S. Song, S. Son, D.Y. Lee, M.-H. Lee, and B.-Y. Kim, *J. Ceram. Process. Res.* 17[11] (2016) 1197-1201.
15. R.-q. Gao, Q. Sun, Z. Fang, G.-t. Li, M.-z. Jia, and X.-m. Hou, *Int. J. Miner. Metall. Mater.* 25[1] (2018) 73-79.
16. R.-q. Gao and X.-m. Hou, *Int. J. Miner. Metall. Mater.* 20[6] (2013) 593-597.
17. S. Qiu, S. Xu, F. Ma, and J. Yang, *Powder Technol.* 210 (2011) 83-86.
18. J. Wang, B. He, and X.Z. Kong, *Appl. Surf. Sci.* 327 (2015) 406-412.
19. T. Georgakopoulos, N. Todorova, K. Pomoni, and C. Trapalis, *J. Non-Cryst. Solids* 410 (2015) 135-141.
20. E.P. Reddy, L. Davydov, and P. Smirniotis, *Appl. Catal., B* 42 (2003) 1-11.
21. S.-y. Lu, Q.-l. Wang, A.G. Buekens, J.-h. Yan, X.-d. Li, and K.-f. Cen, *Chem. Eng. J.* 195-196 (2012) 233-240.
22. B. Wang, G. Zhang, X. Leng, Z. Sun, and S. Zheng, *J. Hazard. Mater.* 285 (2015) 212-220.
23. Y. Chen and K. Liu, *J. Hazard. Mater.* 324 (2017) 139-150.
24. K.-J. Hsien, W.-T. Tsai, and T.-Y. Su, *J. Sol-Gel Sci. Technol.* 51 (2009) 63-69.
25. Z. Sun, Z. Hu, Y. Yan, and S. Zheng, *Appl. Surf. Sci.* 314 (2014) 251-259.
26. Y. Xia, F. Li, Y. Jiang, M. Xia, B. Xue, and Y. Li, *Appl. Surf. Sci.* 303 (2014) 290-296.
27. G. Zhang, Z. Sun, Y. Duan, R. Ma, and S. Zheng, *Appl. Surf. Sci.* 412 (2017) 105-112.
28. C.S. Turchi and D.F. Ollis, *J. Catal.* 122 (1990) 178-192.